ASPIRE: A NEW INDUSTRIAL MWT CELL TECHNOLOGY ENABLING HIGH EFFICIENCIES ON THIN AND LARGE MC-SI WAFERS

Ingrid Romijn, Machteld Lamers, Arno Stassen, Agnes Mewe, Martien Koppes, Eric Kossen and Arthur Weeber
ECN Solar Energy, P.O. Box 1, 1755 ZG Petten, The Netherlands
Tel: +31 224 56 4309, Fax: +31 224 56 8241, Email: Romijn@ecn.nl

ABSTRACT: We present the improved efficiency, and industrial processing of large and thin (<200 µm, 156x156 mm^2) multi crystalline solar cells with silicon-nitride rear side passivation.
The industrial transition towards thinner wafers imposes well known problems for conventional mc-Si solar cells. To maintain high solar cell efficiencies, and reduce the cell bowing on wafers thinner than 200 µm, the full Al rear surface of the conventional mc-Si solar cells has to be replaced by a more appropriate rear surface layer. We apply a single silicon-nitride (SiN_x:H) layer as rear surface passivating layer. An open metallization pattern is applied on both sides of the solar cell using screen printing, and the contacts are co-fired through the SiN_x on front and rear side. The structure of the rear side passivating SiN_x layer has been optimized, as well as the rear surface pre-treatments and metal coverage. This improved processing for rear surface SiN_x passivated solar cells gives a gain in efficiency of almost 1% absolute compared to full Al Back Surface Field, achieving 16.4% on 156 cm^2 240 µm thick mc-Si solar cells. Additionally, a larger batch of 156x156 mm^2, 160 µm thin rear side passivated solar cells have been made using industrial and inline processing, giving an average efficiency of 15.5%, showing that our process is compatible with large area solar cells, and easy to implement into industry.
Taking this new technology one step further, we combine the rear surface passivation with our existing metallization wrap through (PUM) processing. In this new cell concept, ASPIRe, (All Sides Passivated and Interconnected at the Rear), both base and emitter contacts are located at the rear side and the metallization coverage at the front side is reduced by 3% absolute. With this new cell concept, even more drawbacks that arise from processing thinner and larger wafers using the 'standard' cell processing, such as shading and breakage due to front and rear contacting in the module, and losses in FF due to increasing series resistance, are overcome. The ASPIRe cells are made using simple inline processing that can be easily implemented into industry. In this paper, the first results of the new ASPIRe cells will be presented.
Keywords: passivation, bifacial, silicon nitride

1 INTRODUCTION

A general trend to reduce costs for PV is reaching high efficiencies on thin and large solar cells that can be easily mounted into a module. However, processing of thin (<200µm) and fragile wafers using today's technology with full rear surface Al Back Surface Fields (BSF) will reduce the cell efficiency due to non-optimal back-surface passivation and lower internal reflection at the rear side [1-5]. Furthermore, the use of such wafers will cause problems for processing and module assembly due to the increased bowing and breakage. In the past couple of years, several solutions to overcome these bottlenecks have put forward: the usage of bifacial rear side passivated solar cells [1, 2], passivating the rear side with dielectric layers and using laser fired contacts (LFC) at the rear [3], or selective alloying of a local BSF at the rear (i-PERC) [4]. While in the case of bifacial cells only part of the rear surface is covered with metallization, in the case of the LFCs or i-PERC a full Al layer is deposited on top of the passivating layer(s). This full Al layer will increase the fill factor (FF) of the solar cells due to reduction in R_{series}, but remove the possibility of bifacial use and reduction in Al consumption. Our approach towards a new type of solar cells is two-fold:

- First, to increase the efficiency and reduce the bow for thin cells, a SiN_x passivating layer is used at the rear. Open rear metallization of the bifacial cells reduces the cell warping to zero [1,2]. The FF will be improved by optimizing the metallization pattern
- Secondly, the ECN's metallization wrap through (PUM) technology is implemented. This will decrease the shading losses, and minimize losses in FF after interconnection. [6,7,8]. Since all contacts are at the rear side, the thin and fragile cells can be easily assembled into a module using one side interconnection, and thus, resulting in reduced cell breakage in addition to the increase in current.

The two techniques are combined in a new cell concept: the ASPIRe cell (All Sides Passivated and Interconnected at the Rear cell). The ASPIRe cells are made using only inline processing that can be easily implemented into industry.

Passivated back contact technologies, such as ASPIRe, will pave the way for future inline cell processing of thin and large high-efficiency mc-Si solar cells. The technology combines several techniques and process steps that have already been developed and proven at ECN such as rear surface passivation [2] and PUM processing [8], while also incorporating newly developed inline process steps to structure the rear surface of the cells.

In the first part of the paper, we focus on optimizing the rear surface passivation, and bifacial H-patterned solar cells (fig 1a). In the second part of the paper, our first working ASPIRe cells are presented and discussed (fig 1b). The solar cells were processed using both relatively thick (240 µm) and thinner (180 µm) mc-Si wafer material.

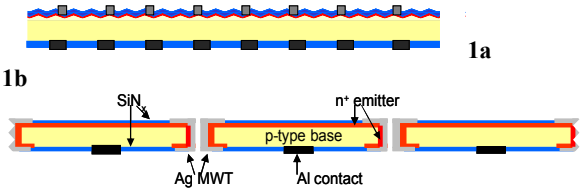

Figure 1a and b: Cross-section of our bifacial cell (a) and the new ASPIRe cell (b): Red: emitter; blue: SiN_x coating; grey: Ag (in ASPIRe: front, in holes and locally on rear) and black: Al (local rear) metallization.

2 APPROACH

The consecutive steps towards our new ASPIRe cell concept are:

1. First, the processing of our bifacial cells is optimized in efficiency and readied for industrial implementation. This is done by:
   - development and optimization of a dedicated rear surface passivating layer
   - detailed analysis of the passivating layers on cell level
   - optimizing the solar cell processing for large and thin wafers, while using the conventional H-pattern metallization on both front and rear side
2. Secondly, the additional processing steps for the ASPIRe cells are investigated. The largest differences between the 'standard' bifacial solar cells and the ASPIRe cell are the (16) holes through the wafer and the local emitters at the rear side.

All experimental steps and results will be discussed in separate paragraphs below.

3 EXPERIMENTS, RESULTS AND DISCUSSIONS

3.1 Development and optimization of the SiN_x rear side passivation

A general rule for single SiN_x layers is that the surface passivation improves when the layer becomes less dense, and contains more Si-Si and hydrogen bonds and less Si-N bonds [9,10]. The optimal passivating layers generally have a high refractive index (up to n=2.5), and a higher H-content. This type of SiN_x layers is usually not applied on the front surface of solar cells, high refractive index will cause an increased absorption at lower wavelengths. However, when the layers are applied on the rear side of the solar cells, the additional absorption lower wavelengths will not hinder the cell efficiency. Another possible problem is that if these layers have a too low density, their thermal stability decreases, giving rise to high recombination velocities after the high temperature (firing) step that is necessary to contact screen printed metallization.

We have developed a SiN_x layer with a high refractive index (n=2.5) and low Si-N bond density ($0.9*10^{23}$ cm^{-3}) that contains a high amount of Si-H bonds and is still thermally stable up to the temperatures used for firing of the metallization.

In figure 2 recombination velocities (S_{eff}) of this "dedicated rear surface" passivating layer, our standard front side SIN_x layer with n=2.1 and Si-N = $1.3*10^{23}$ cm^{-3} and two stacked layers (SiN_x/SiN_x and SiO_x/SiN_x) are shown. The SiN_x/SiN_x stacked layer is added because even though the dedicated rear sided layer gives better surface passivation, the SiN_x/SiN_x stack might enhance the bulk passivation of mc-Si solar cells due to the denser SiN_x on top [11], which might prevent out-diffusion of hydrogen. The SiO_x/SiN_x stacked layer is added because it might perform better than pure SiN_x layers on the rear of solar cells due to, for instance, a lower amount of fixed charges [12,13].

All layers were deposited on both sides of 1 Ω-cm polished float zoned (FZ) wafers. All single SiN_x layers were ~80 nm thick. The SiN_x/SiN_x stacked layer consisted of a 40 nm lower density SiN_x, capped by 40 nm of the more dense front side SiN_x. The SiO_x was also capped by the dense front side SiN_x.

The effective lifetimes (τ_{eff}) of the samples were measured using Quasi Steady State Photo Conductance method [14]. Recombination velocities (S_{eff}) were calculated using the approximation: $1/\tau_{eff} = 1/\tau_{bulk} + 2S_{eff}/W$, with W the thickness of the FZ wafer [15]. τ_{bulk} is assumed to be 1 ms for the FZ material.

The recombination velocities all remained below 20 cm/s after firing, as can be seen in figure 2. Surprisingly, while the single layers improved after firing (front side SiN_x), or remained stable (dedicated rear SiN_x), while the stacked layers (both SiN_x and SiO_x) increased in recombination velocity after firing.

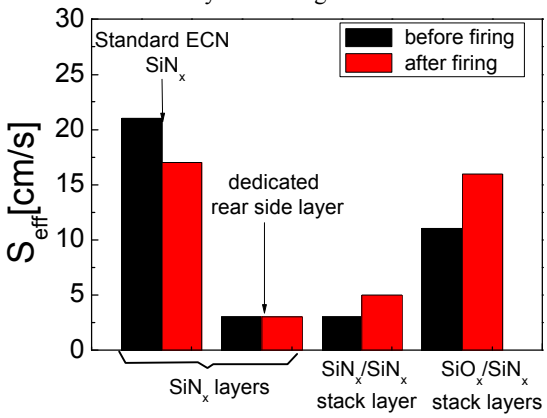

Figure 2: Recombination velocities of different silicon oxide and silicon nitride coatings, before and after firing. The ECN Baseline SiN_x layer is used for the front side of the solar cells. The dedicated rear side SiN_x layer was especially optimized for rear side coatings.

3.2 Optimizing bifacial solar cells

3.2.1 Processing and testing of the different rear surface layers

P-type mc-Si neighboring wafers (240 µm thick, 125x125 mm^2) were processed using the sequence shown in figure 3. After the wet-chemical iso-texturization, 65 Ω/sq emitters were diffused using an inline belt furnace. To prepare the rear surface for optimal passivation, the rear side emitter was removed and the rear surface cleaned and smoothened for better passivation. The standard ECN SiN_x coating [16] was used for all front sides of the solar cells in the experiments, while the four different passivating layers shown in figure 2 were applied on the rear surface of groups of neighboring wafers. An H pattern Al metallization was used for rear side contacting and local BSF formation. The Aluminium paste used was specially developed to enable firing through the SiN_x on the rear side. Both the Ag front and Al rear contacts were fired through the SiN_x layers in a single co-firing step. Because the emitter on the rear surface is removed in step 4 (fig 3), no edge isolation (e.g. laser) is needed. Thus, effectively only one additional process step, the second SiN_x layer, is needed with respect to the conventional mc-Si processing. This means that the process can be easily implemented into industry.

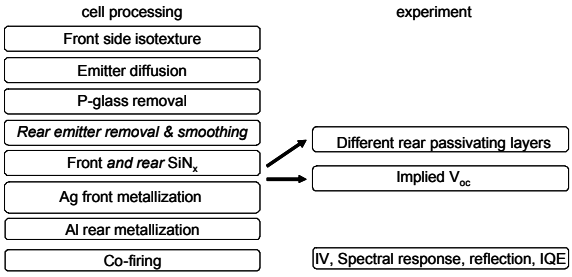

Figure 3: Flow chart of processing of and experiments on rear side passivated solar cells

Implied V_{oc} was measured on mc-Si wafers for all groups before and after a firing step, without any metallization, as a measure of both bulk and surface passivation. The $V_{oc,imp}$ values at 1 sun illumination were extracted from the injection dependent lifetime measurements [14]. Averaged results of 5 wafers per layer are shown in figure 4. Implied V_{oc}'s of > 660 mV were achieved after firing for wafers passivated with the dedicated rear surface layer. The results are similar to those already obtained for the surface passivation on FZ material: the dedicated rear surface SiN_x layer gives the highest implied V_{oc}, thus the best passivation. Both single SiN_x layers improve after firing, while the stacked layers give a decreased implied V_{oc} after firing. The deposition of a thinner layer underneath the dense SiN_x apparently reduces the firing stability. A possible explanation might temperature induced stress between the layers.

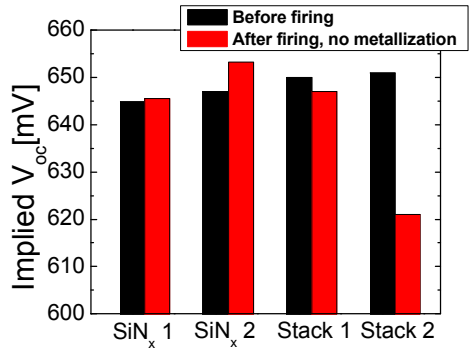

Figure 4: Average implied V_{oc} results for different rear surface passivating layers. Rear surface is smoothened

IV characteristics of the complete solar cells were measured using our Class A solar simulator according to the ASTM-E948 norm, full area Internal Quantum Efficiency (IQE) was calculated from spectral response and reflection measurements. The averaged results for J_{sc} and V_{oc} with different rear surface passivating layers, including a full Al rear surface reference group, are shown in figure 5 and table I. The final values for V_{oc} after complete processing are about 40 mV lower than the implied V_{oc} measured. This is due to the additional handling, metallization steps and the firing of the Al pattern through the rear side passivating coating. However, the difference in passivation, as measured in implied V_{oc} before metallization is clearly reflected in the values for J_{sc} and V_{oc} for the different groups, giving maximum values for both J_{sc} and V_{oc} for the dedicated rear side passivation. The current obtained with the dedicated rear SiN_x (35 mA/cm^2, see table I) is ~3% higher than the J_{sc} of the Al reference (33.9 mA/cm^2), although the V_{oc} (609 mV) is similar to the reference value of 607 mV. This indicates that J_{sc} is most susceptible to fine-tuning of rear surface optimization. This is confirmed by PC1D analysis, as will be shown below.

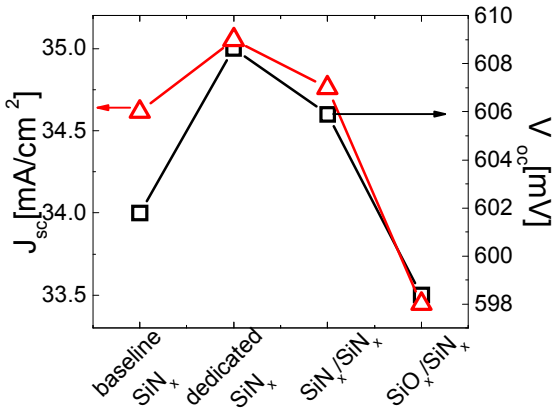

Figure 5: Average IV results for different rear surface passivating layers, applied on a smoothened rear surface

Table I: IV results of the bifacial solar cells

Rear Side	J_{SC} (mA/cm^2)	V_{OC} (mV)	FF (%)	η (%)
Full Al	33.9	607	75.6	15.5
SiN_x-1	34.0	606	73.2	15.1
SiN_x-2	35.0	609	75.4	16.1
(max)	(35.2)	(611)		
Stack-1	34.6	607	74.5	15.6
Stack-2	33.5	598	73.3	14.7
Top cell (SiN_x-2)	35.0	609	77	16.4

3.2.2 Detailed analysis of cell results

To obtain more knowledge on the difference between the several groups of solar cells, the internal quantum efficiency (IQE) is obtained from full area spectral response and reflection measurements of the solar cells. Using PC1D [17], both the IQE measurement and IV results can be fitted simultaneously, giving values for front side (internal) reflection, front side recombination velocity and emitter doping, bulk lifetime τ_{bulk}, rear side recombination velocity ($S_{eff,rear}$) and rear side (internal) reflection. Since we are focusing on the rear side of the solar cells, the main parameters of interest are the rear side recombination velocity $S_{eff,rear}$ and rear side reflection R_{rear}. If only the IQE measured from the front side is available it is very hard to distinguish between the different contributions of τ_{bulk} and $S_{eff,rear}$. However, due to the open rear metallization, we are able to obtain IQE measurements from both the front and rear side of the solar cell. If the IQE obtained from the rear side is fitted simultaneously with the IQE obtained from the front side, the contributions of τ_{bulk} (800-1000 nm in both front- and rear-IQE) and $S_{eff,rear}$ (600-900 nm in rear-IQE, 800-1000 nm in front-IQE) can be separated. Using PC1D, one has to keep in mind that it is a 1-dimensional model. Because of the front side texturization, the solar cells should be fitted with a 2-dimensional device simulation model to be more physically correct. However, the PC1D-fitted values of the parameters such as $S_{eff,rear}$ and R_{rear} with respect to each other will be correct, even though the absolute values are approximations.

Except for the full Al rear surface cells, the internal quantum efficiency measurements from the rear side of the solar cells with different rear side passivation schemes are shown in figure 6, including the fits from the PC-1D analysis.

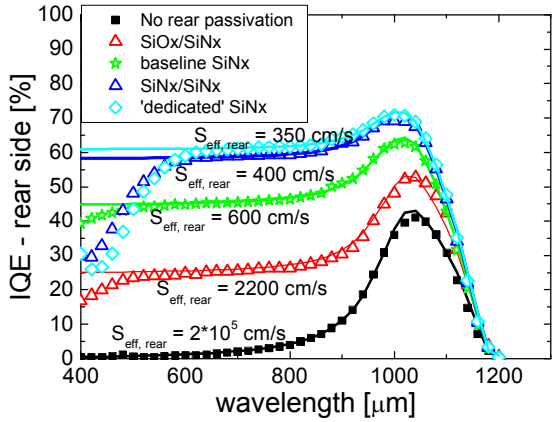

Figure 6: IQE measurements and PC1D fits from the rear side of the solar cells. For the lower wavelengths (<500nm) the results are affected by the absorption in the passivating layers. This causes a lower IQE, even though the surface passivation is good. When the cell is illuminated from the front, this absorption at lower wavelengths at the rear will not hinder the cell efficiency.

Since all the groups were made of neighbouring material values for τ_{bulk} are similar, around 25-30 µs. Also the front parameters such as front surface passivation (2.5*10^5 cm/s) and reflection (85%) were the same for all groups. A lowest value of $S_{eff,rear}$ = 350 cm/s is obtained for the cells passivated with the 'dedicated' single SiN_x layer.

In figure 7, both the front- and rear-IQE of a rear-passivated mc-Si cell (using dedicated rear-SiN_x) are shown together with the front-IQE of the full Al reference cell. At 1000 nm, the two front-IQEs are overlapping. This means that the full Al rear solar cell has similar low rear surface recombination velocities (fitted with PC1D to $S_{eff,rear}$ ~350 cm/s) as the rear side passivated solar cell [16]. Such low recombination values for BSF's are not usually obtained in industry, where the values for $S_{eff,rear}$ are usually above 1000 cm/s [5]. Above 1000 nm however, there is a clear enhancement in the front-IQE of the rear side passivated cell compared to the Al reference. This gain is due to the enhancement in rear reflection for SiN_x coatings compared to the full Al rear side -PC1D fits give R_{rear} = 72% for the Al reference versus 85% for the SiN_x- and is reflected in the increased J_{sc}.

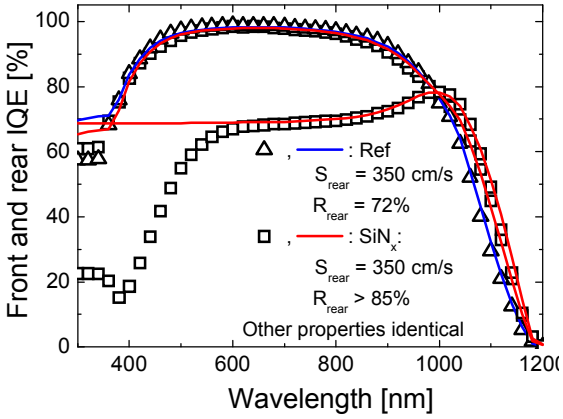

Figure 7: front and rear IQE of a rear side passivated (using dedicated SiN_x) solar cell, and front IQE of a full Al rear solar cell.

3.2.3 Larger and thinner wafers

For p-type wafers with a bulk lifetime τ_{bulk} of 25 µs, the diffusion length D_l is around 280 µm. When the wafers become thinner (or the τ_{bulk} larger), the rear surface of the solar cells becomes more and more important. Also the bowing of the thinner wafers will be more enhanced for full area Al BSF solar cells.

When the wafers become larger (156x156 mm^2 in stead of 125x125 mm^2) another issue has to be addressed besides the rear surface passivation: the amount of (open) metallization at the rear. The total recombination velocity ($S_{eff,total}$) on the rear side is determined by both the recombination velocity of the SiN_x ($S_{eff,SiNx}$) and the recombination velocity of the local BSF below the metallic (fired through) contacts ($S_{eff,metal}$). The local BSF below the metal contacts ($S_{eff,metal}$ ~ 500-1000 cm/s) will not be good as the BSF of a full Al covered solar cell (S_{eff} ~ 350 cm/s). This is because the printed lines will broaden during drying and firing, causing less Al/cm^2. Moreover, the firing through SiN_x will hinder some of the formation of the local BSF.

If the percentage of metal coverage becomes larger, the total $S_{eff,rear}$ becomes dominated by $S_{eff,metal}$, and both V_{oc} and J_{sc} will drop. However, when the metal coverage becomes too small, the series resistance will increase (for instance increase in R_{serie} due to finer lines) and the FF will drop. Because of the larger generated current, and longer length of the fingers, this problem is more explicit for 156x156 mm^2 than for 125x125 mm^2 wafers. Thus, for larger cells we expect to have either good passivation and low FF, or 'bad passivation' and high FF. The challenge for these large, rear side passivated solar cells is to minimize the metal coverage on the rear, while maintaining a good FF.

The cell processing described in the previous paragraph, using our dedicated SiN_x, was applied on 156x156 mm^2, 160 µm thin wafers. Within this batch, the metal coverage on the rear was varied from 10% (as it was in the 125x125 mm^2 solar cells) to 20%.

As can be seen from figure 8, the metal coverage has a large influence on the rear surface passivation as seen in the rear IQE and consequently on both V_{oc} and J_{sc}. The highest values for V_{oc} and J_{sc} (608 mV and 34.3 mA/cm^2) were obtained for the group with 10% metal coverage, compared to 605 mV and 33.8 mA/cm^2 for the fully Al covered reference. However, the solar cells with only 10% rear side metallization had a too low FF (<70%) to

obtain high efficiencies. For all other cells high FF (>75%) could be reached. Even though the values for J_{sc} and V_{oc} were not as high as for those with less metal coverage (J_{sc} = 34.0 mA/cm^2 and V_{oc} = 605 mV), still efficiencies of 16% were reached, with an average efficiency of 15.5%.

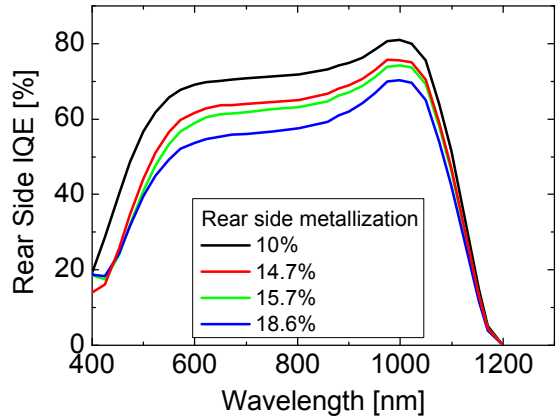

Figure 8: Rear IQE for different metallization coverage on the rear side

A large batch of these thin wafers was processed, to test the industrial applicability of the process flow. The results for 60 wafers with metallic coverage between 14 and 16% are shown in figure 9. Also the full Al BSF reference cells are shown (less wafers were processed for the reference). It is clear, that although the metallization pattern at the rear is not yet fully optimized with respect to R_{serie} and passivation and gives a reduction in both V_{oc} and J_{sc}, the processing is relatively stable and gives an efficiency distribution that is 0.4% absolute higher than the reference, full Al covered process. The maximum efficiency reached is 16.1%. On top of this, the bowing is reduced to zero for the bifacial cells, compared to >2 mm for the reference cells.

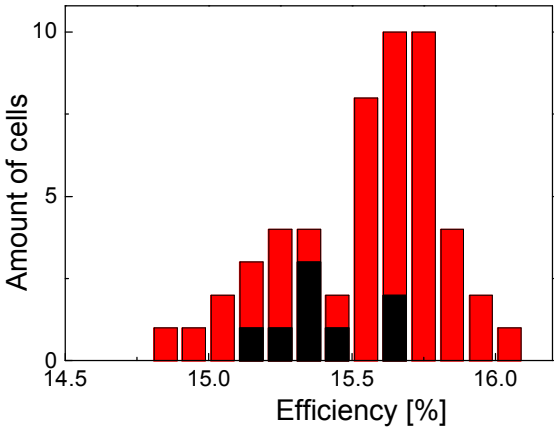

Figure 9: Red: the efficiencies of 60 156x156 mm^2, 160 µm thick rear side passivated solar cells with metallic coverage between 14 and 16%. Black: 10 reference full Al cells (neighboring wafers)

Some authors have found evidence that single SiN_x layers would not be good enough for the rear surface passivation of p-type mc-Si solar cells. This would be due to for instance parasitic shunts caused by fixed charges in the Si-SiN_x interface [12,13]. We find that – at least down to $S_{eff,rear}$ of 350 cm/s - this is not limiting the efficiency of large and thin solar cells [2]. Furthermore, we have found that single SiN_x layers can be good as, or even better than, stacked dielectric layers [3,4] for the passivation of bifacial solar cells.

3.3 New processing steps for the ASPIRe cells

As was mentioned in the introduction, the second step towards our new ASPIRe cell concept is to combine the existing ECN-PUM concept with our optimized rear side passivated solar cell (see fig 1a and 1b). During recent years, ECN has developed the PUM cell to minimize the front side metallization coverage and improve the FF (especially after encapsulation). Moreover, the PUM and ASPIRe cells are fully back contacted solar cells, which means they can be easily assembled ('pick and placed') into a module[6,7,8].

Besides the rear surface passivation, ASPIRe cells have a local emitter around the holes at the rear, and therefore require additional processing. We have tested several solutions for this local processing. Two of these were:

1) Use of diffusion barrier. In this case, the rear surface is smoothened before emitter formation. A screen printable diffusion barrier is applied to enable local emitter formation around the holes. The barrier is removed during the PSG removal step.
2) Selective removal of the emitter and smoothening of the rear surface after diffusion. Again, the remainder of the processing is similar to that of the bifacial H-pattern solar cells.

Both processing methods are shown in the flow chart in figure 10.

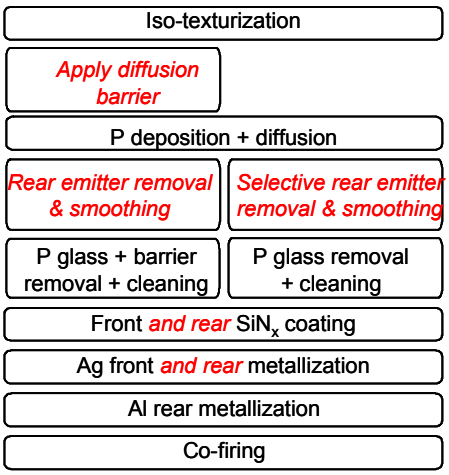

Figure 10: Flowchart of two possible processing methods of the ASPIRe cells. In red text are the additional processing steps needed compared to standard cell processing

Besides the advantages of better passivation and no bow compared to full Al BSF cells (H-patterned or PUM), problems arising from the rear side passivation and metallization of large solar cells (either good passivation and low FF, or 'bad passivation' and high FF, see paragraph 3.2.3) can be solved by using the ASPIRe concept. Due to the modular design (see fig 11), the FF can be optimized for less rear side metallization.

In figure 11 the front and rear metallization pattern of the ASPIRe cells is shown. The front side pattern is the same as for our standard PUM cells.

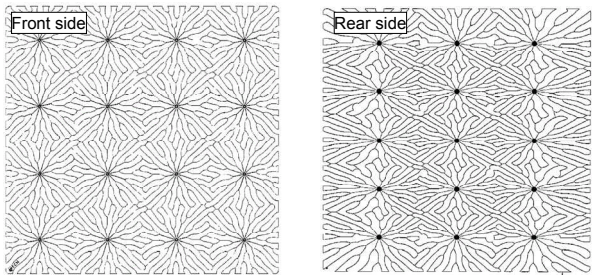

Figure 11: front and rear side, and cross section of the ASPIRe cell. Metallization pattern courtesy to Solland Solar BV

The rear pattern shown is only the base metallization pattern (Al), the rear Ag emitter contacts are added in a separate printing step. When mounted into a module, the interconnection of the cells only takes place at the rear side, where both the emitter and base contacts are located. Both contacts can be seen in the photo of the rear side of the first finished ASPIRe cell in figure 12.

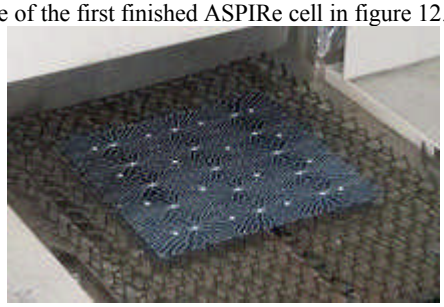

Figure 12: photograph of the rear side of the first ASPIRe cell. Both emitter and base contacts are clearly visible

The first results of the ASPIRe cells and their bifacial H-pattern reference are shown in table II. All ASPIRe cells were processed on 160 µm thin, 156x156 mm^2 material.

Table II: IV results of the first batch of ASPIRe cells

		J_{sc} (mA/cm^2)	V_{oc} (mV)	FF (%)	Eta (%)
Diffusion barrier	Avg	33.3	599	67	13.1
	Max	34.0	604	70	14.3
Emitter removal	Avg	34.1	604	71	14.5
	max	34.5	609	71	14.8
Improved metallization	Avg	34.5	609	74	15.6
	max	34.6	609	75	15.9
Bifacial ref		33.6	602	77	15.5

The first results from ASPIRe are very promising: values for J_{sc} ~ 34.6 mA/cm^2 and V_{oc} ~ 609 mV were achieved. The efficiency is 0.4% higher for ASPIRe than for the reference, reaching 15.9%. The average values for $J_{sc}*V_{oc}$ of the ASPIRe cell processed with the second method lie ~3% relative higher than those of their bifacial H-references. This gain is mainly due to the increased current, and caused by the lower amount of front metallization. Also the V_{oc} is improved compared to the H-patterned reference. This is probably due to a better rear surface passivation, since also the rear metallization coverage is less for the ASPIRe cells (ASPIRe ~ 10%, H ~ 16%). More analysis is needed to quantify these parameters. Also the specific differences between the different process flows for the ASPIRe cells need to be analyzed in more detail.

The total rear surface metallization of the ASPIRe cells was about 10%, indicating that even without optimization the ASPIRe is already advantageous over the H-pattern solar cells. For these solar cells the FF remained below 70% for 10% metallization (see paragraph 3.2.1), whereas the ASPIRe reaches 75%.

Small modules will be made from these ASPIRe cells to test the interconnections. Eventually, the ASPIRe cells are going to be mounted into a module using newly developed interconnection techniques, such as conductive adhesives [7,8].

4 CONCLUSIONS

In this paper we present rear side SiN passivated bifacial solar cells and our new cell concept ASPIRe: All Sides Passivated and Interconnected at the Rear cell. A highest efficiency of 16.4% was reached on bifacial cells made from 240 µm, 125x125 mm^2 mc-Si material, with 3% higher J_{sc} and similar V_{oc} than the full Al BSF reference cells. The gain in J_{sc} is mainly due to the enhanced optical confinement from the rear SiN_x, while the V_{oc} is governed by the rear surface recombination velocity $S_{eff,rear}$. Lowest $S_{eff,rear}$ of 350 cm/s were reached. In industry, usually values of ~1000 cm/s are reached with Al BSF, which means passivation by SiN_x should easily give an increase in both V_{oc} and J_{sc}. These increases will become even more significant when the wafers become thinner than 200 µm, and the rear surface passivation will be even more important.

For ASPIRe cells, the advantages of rear surface SiN_x passivation are combined with the benefits of our existing MWT-PUM technology. A new inline process is developed to allow local emitter formation on the rear surface. The first results from ASPIRe are very promising: values for J_{sc} ~ 34.6 mA/cm^2 and V_{oc} ~ 609 mV were achieved, 3% relative higher than their bi-facial H-references. Maximum efficiency obtained so far is 15.9%.

5 ACKNOWLEDGEMENTS

This work was financially supported by the FP6 European Crystal Clear project (EC contract SES6-CT-2003-502583) and by the Dutch Senter Novem project StarFire (EOS-ES program project IS063024). Partners are gratefully acknowledged for their helpful discussions. Solland Solar Energy BV is acknowledged for using the metallization pattern of the ASPIRe cells

6 REFERENCES

[1] L. Janssen et al., Progress in Photovoltaics: Res and Appl 15, 2007, 469-475
[2] I. G. Romijn et al., Proceedings 21st EPVSEC, Dresden, September 2006, 717
[3] M. Hofmann et al., Proceedings 21st EPVSEC, Dresden, September 2006
[4] G. Agostinelli et al., Proceedings 21st EPVSEC,

Dresden, September 2006; Proceedings 20st EPVSEC, Barcelona, September 2005
[5] C. J. J. Tool et al., Solar Energy Mat. and Solar Cells 90, 2006, 3165-3173
[6] J. H. Bultman et al., Proceedings WCPEC-3, Osaka, 2003
[7] P. C. de Jong et al., Proceedsngs 19th EPVSEC, Paris, June 2004, 2145
[8] A. W. Weeber et al., Proceedings 21st EPVSEC, Dresden, September 2006, 605
[9] H. Mackel and R. Ludemann, J. Appl. Physics 92, 2002, 2602
[10] I. Romijn et al., 15th Workshop on crystalline silicon solar cells & modules: Materials and Processes, Vail, colorado, 2005, 82-85
[11] H.F.W. Dekkers, Proceedings 20th EU PVSEC, Barcelona, June 2005
[12] S. Dauwe, L. Mittelstädt, A. Metz, R. Hezel, Progress in Photovoltaics, Res. And Appl., 10, 271-278, 2002
[13] O. Schultz et al., Proc. Proceedings WCPEC-4 Hawaii 2006
[14] R. A. Sinton and A. Cuevas, Appl, Phys. Lett 96, 1996, 2510
[15] M. Greene, Solar Cells, operating principles, UNSW, Australia, 1982
[16] C.J.J. Tool et al., Proc. 20th EU PVSEC, Barcelona, June 2005
[17] P.A. Basore, D.A. Clugston, PC-1D v5.5, University New South Wales 2000